# 21. On Dispersion Curves of Surface Waves from the Great Assam Earthquake of September 15, 1950.

By Tetsuo AKIMA,

Earthquake Research Institute.

(Read June 17, 1952.—Received June 20, 1952.)

## 1. Introduction.

Many authors have already studied the propagation of seismic surface waves[1]. The dispersion curves for Love-type or Rayleigh-type waves along various paths of propagation, such as the Pacific, the Atlantic, the Indian Oceans, or the continents of Eurasia and America etc., have separately been obtained by them. None has, however, succeeded in obtaining the dispersion curves of both Love and Rayleigh waves with respect to one and the same earthquake.

On September 15, 1950, a great earthquake took place in Assam district in India. The epicenter of the earthquake was located at $\lambda=28°.6\text{N}$, $\varphi=96°.5\text{E}$. The seismic waves of this earthquake were reported to have been well recorded by almost all the seismographs in the world. Records of the seismic waves of this earthquake were also obtained by Wiechert-type seismographs working at a number of Meteorological Observatories in Japan.

This great earthquake gave the writer a good opportunity to obtain both of these two dispersion curves. Since, as is seen in Fig. 1, the paths of seismic waves from the origin to the observatories in Japan have

1) For instance,
G. ANGENHEISTER, *Nachr. d. Kgl. Ges. d. Wiss. Gött., Heft* **1** (1906).
F. ROESENER, *Gerl. Beitr. Geophys.*, **12** (1913).
B. GUTENBERG, *Phys. Zeit.*, **25** (1924), 377.
T. MATUZAWA, *Bull. Earthq. Res. Inst.*, **6** (1929), 214.
P. BYERLY, *Gerl. Beitr. Geophys.*, **26** (1930).
W. ROHRBACH, *Zeit. für Geophys.*, **8** (1932), 113.
W. MÜHLEN, *Zeit. für Geophys.*, **8** (1932).
D. S. CARDER, *Bull. Seis. Soc. Amer.*, **24** (1934), 231.
J. T. WILSON, *Bull. Seis. Soc. Amer.*, **30** (1940), 273.
J. F. De LISTLE, *Bull. Seis. Soc. Amer.*, (1941), 303.
J. T. WILSON and O. BAYKAL, *Bull. Seis. Soc. Amer.*, (1948), 41.

almost E–W direction, Love and Rayleigh waves are expected to be separately recorded on seismograms of N–S and W–E or U–D components at each observatory respectively.

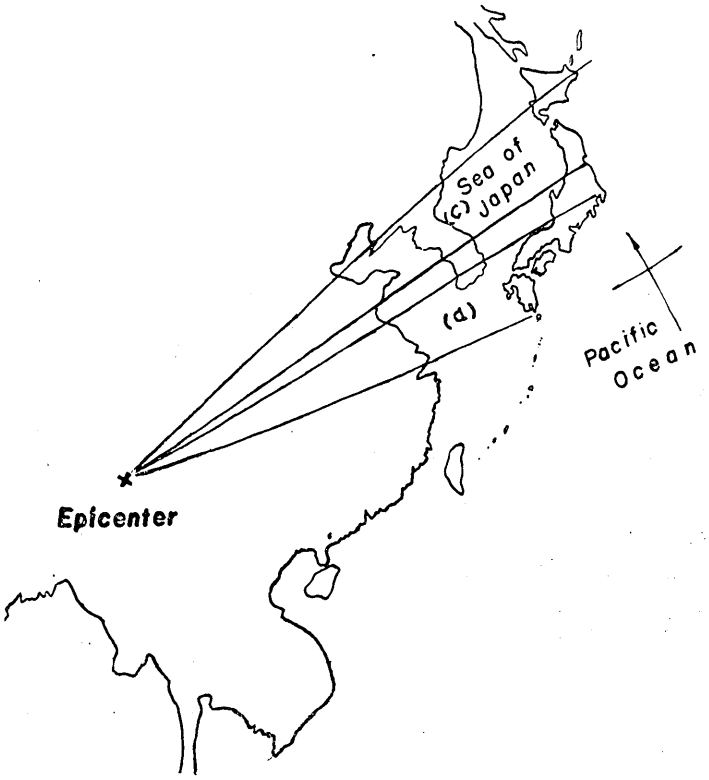


Fig. 1. The paths of wave propagation from the epicenter to the observatories in Japan.

## 2. Filtering of seismorgrams.

Short period waves recorded on seismograms make it pretty difficult to study the surface waves alone. Fig. 2 shows examples of such seismograms. Though a few series of long waves are recognizable on these seismograms, the onsets or the latter parts of the series are very obscure, being largely effaced by short period waves.

In order to observe clearly the long period waves involved in these seismograms by eliminating the short period waves, a torsion pendulum low-pass filter which was constructed by the writer was used[2]. Several

2) T. AKIMA, *Bull. Earthq. Res. Inst.*, **30** (1952), 53.

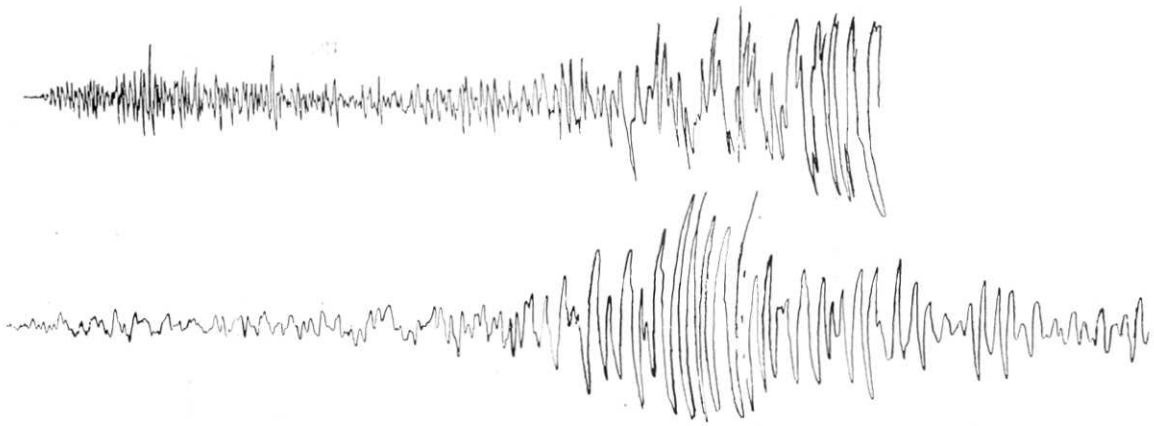

Fig. 2. Examples of seismograms.

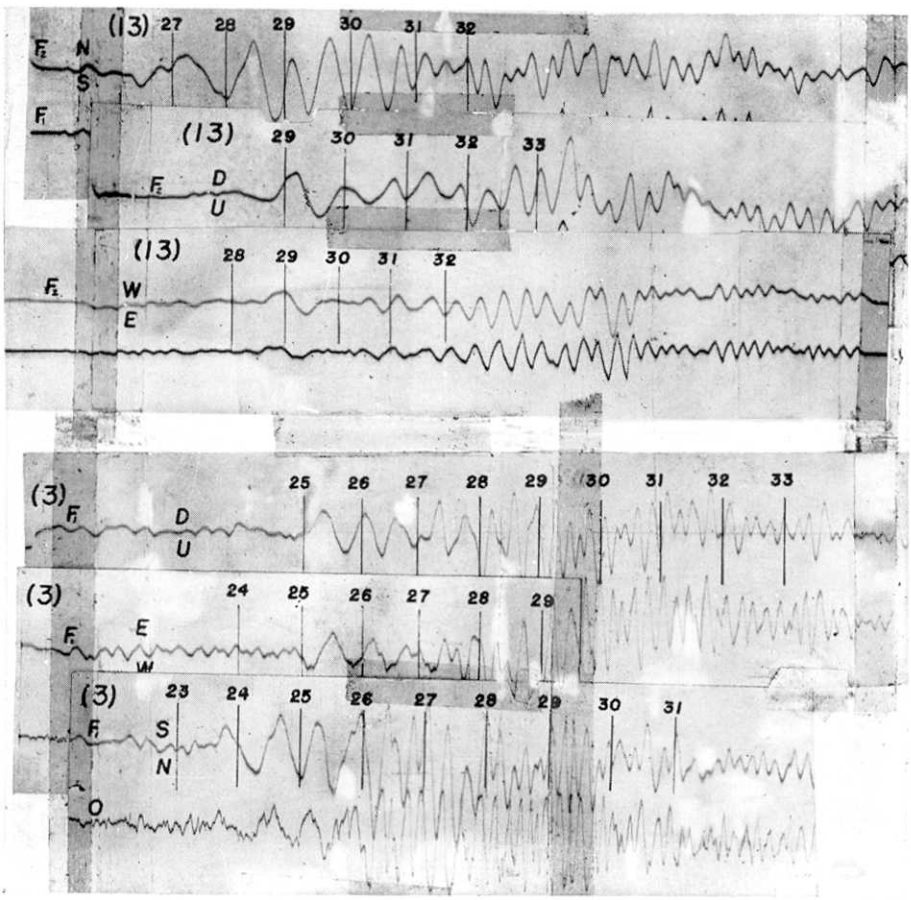


Fig. 3. Examples of the filtered record representing the separated Love and Rayleigh waves.

examples of the records after filtration are shown in Fig. 3, in which $O$, $F_1$, $F_2$ and $F_3$ denote the original, once-, twice- and thrice- filtered waves respectively. The times indicated in this figure are minutes in G.M.T.

### 3. Confirmations of Love and Rayleigh waves.

In these long period waves which remain after filtration, the arrival times and the periods of the first waves were measured at first. In measuring the arrival times of waves, the time lags of the motion of the torsion pendulum were of course taken into account and were reduced to the original times. The time intervals between the onset times and the times of the next occurrence of the same phases were taken as the periods of these waves. The results of readings are given in Table I. From this Table and Fig. 3, the arrival times of long period waves of E–W components are evidently almost the same as those of U–D

Table I.

| | $\Delta$ in km | $P$ | $L$ | | | $T_L$ | | | $\frac{T_{EW}}{T_{NS}}$ | $\frac{T_{UP}}{T_{NS}}$ |
|---|---|---|---|---|---|---|---|---|---|---|
| | | (G.M.T.) | $EW$ | $NS$ | $UD$ | $EW$ | $NS$ | $UD$ | | |
| 1. Nagasaki | 3220 | h m s 14 15 27.3 | | m s 23 20 | | | s 51 | | | |
| 2. Yakusima | 3293 | 〃 34.5 | m s 24 50 | 23 25 | m s 24 55 | s 46 | 52 | s 46 | 0.89 | 0.89 |
| 3. Hukuoka | 3280 | 〃 36.3 | 24 50 | 23 42 | 24 50 | 47 | 52.5 | 47 | 0.90 | 0.90 |
| 5. Ôita | 3285 | 〃 47.1 | 25 41 | 24 12 | | | 54 | | | |
| 6. Simizu | 3500 | 〃 56.4 | | | 26 17 | | | 42 | | |
| 7. Hamada | 3450 | 〃 48.9 | 25 25 | 24 05 | | 50 | 53 | | 0.94 | |
| 8. Kôti | 3560 | 〃 48.2 | 25 30 | | | 49 | | | | |
| 9. Sumoto | 3700 | 16 08.9 | | | 26 30 | | | 50 | | |
| 10. Ôsaka | 3760 | 〃 13.5 | 26 25 | 24 25 | 26 42 | 48 | 55 | 54 | 0.87 | 0.98 |
| 11. Gihu | 3865 | 〃 21.8 | 27 25 | 26 00 | | 51 | 57 | | 0.90 | |
| 12. Tôkyô | 4080 | 〃 41.5 | | 27 30 | 28 45 | | 57 | 52 | | 0.91 |
| 13. Tukubasan | 4080 | 〃 43.8 | 28 30 | 27 25 | 28 50 | 57 | 56 | 52 | 1.02 | 0.93 |
| 14. Morioka | 4275 | 〃 54.2 | 29 00 | 27 35 | 29 05 | 52 | 57 | 51 | 0.91 | 0.90 |
| 15. Sendai | 4250 | 〃 49.1 | 29 00 | 27 30 | 29 05 | 51 | 60 | 52 | 0.85 | 0.87 |
| 16. Sapporo | 4330 | 〃 | | | 28 25 | | | 53 | | |
| 17. Nemuro | 4670 | 17 20.5 | 31 30 | 29 05 | | 50 | 58 | | 0.86 | |

$P$: Arrival times of $P$ waves.
$L$: Arrival times of surface waves in each component.
$T_L$: Periods of surface waves in each component.
$T_{EW}/T_{NS}$: Ratios of period of Rayleigh and Love waves in $E$-$W$ and $N$-$S$ component.

components, while they are considerably later than those of N–S components. This fact suggests that the long waves which are seen in the filtered records of N–S and E–W or U–D components correspond to Love and Rayleigh waves respectively. In order to make sure of this supposition, the dispersive character of these long period waves was investigated. The arrival times and periods of the waves which followed were measured on each filtered record. The method of measuring is illustrated schematically in Fig. 4, in which the times of $a_1$, $b_1$, $a_2$, $b_2$, etc. were taken as the arrival times of waves with the periods corresponding to the time differences of $a_2-a_1$, $b_2-b_1$, $a_3-a_2$, $b_3-b_2$, etc. respectively.

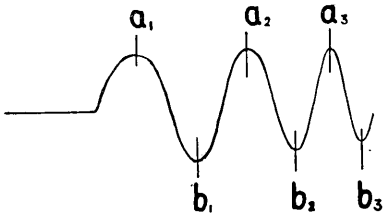

Fig. 4.

Figs. 5–a, –b, –c represent the relations between the periods and the arrival times of the filtered long waves in each component. The numbers given on both ends of each curve indicate the position numbers of the observatories whereby the curves were obtained. (cf. Fig. 8). Though the examples given here are limited in number, they clearly show the dispersive character of the waves, i. e. the longer period waves have greater velocities. In these figures, it can be seen that some points, marked by hollow circles, do not lie on the smooth trend of the curves. The discussion for these points will be given later.

The orbits of the ground motions due to the long period waves recorded as E–W and U–D components at each observational position were next calculated in order to see whether the waves appeared in these components are Rayleigh-type waves or not. Fig. 6 shows the results for the observatories Nos. 2, 3, 10, 13, 14 and 15. The double-feathered arrows show the directions of wave propagation and the numbers given on each curve denote the times in minutes reckoned from the beginings of the long period waves. Except for the earlier part of the orbit at the station No. 10 (Ôsaka), all show the retrograde nature of the motions, which makes it certain that the filtered long period waves on E–W and U–D components are Rayleigh waves.

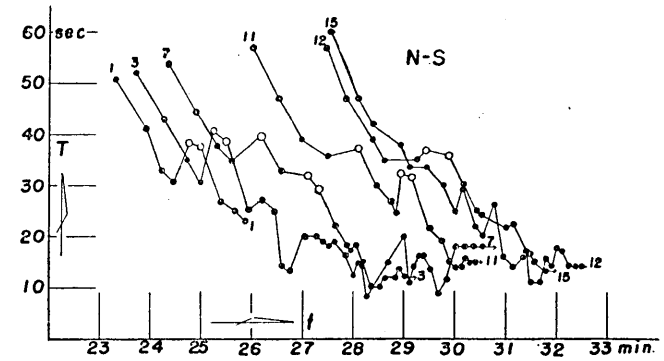


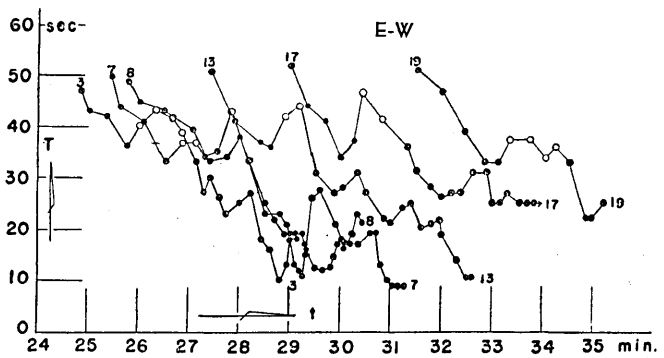


b.

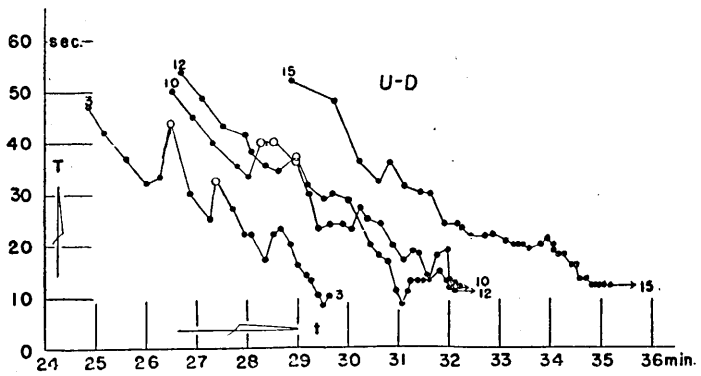


c.

Fig. 5. Relations between the arrival times and the periods of the filtered waves. a. N-S, b. E-W, c. U-D

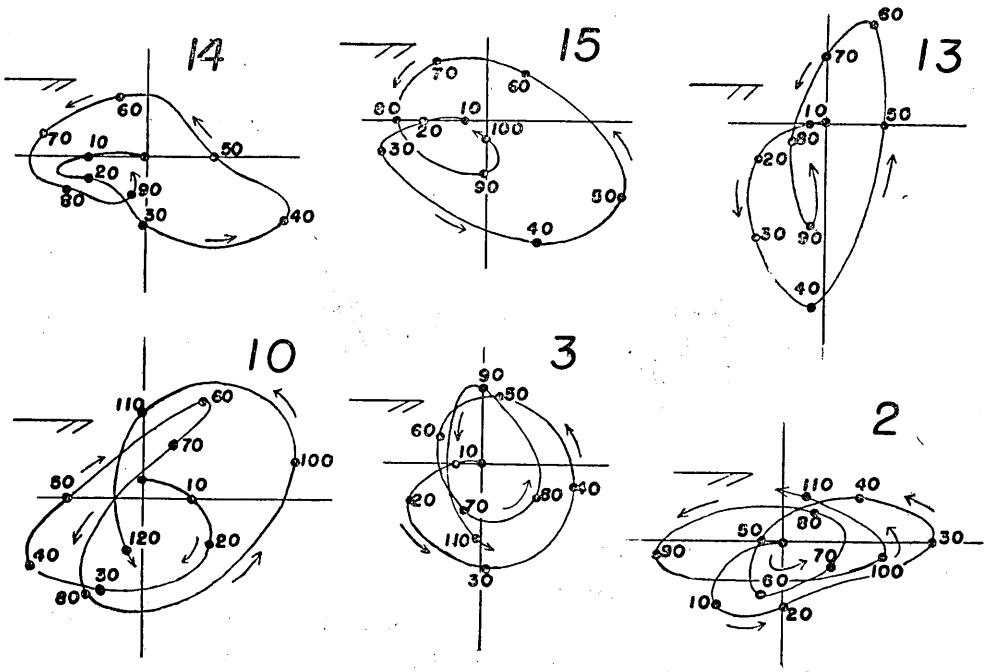


Fig. 6. Retrograde nature of the ground motions due to the filtered long period waves.

## 4. Dispersion curves.

Owing to the favourable positions of observatories in Japan with respect to the direction of wave propagation of this great earthquake and with the aid of the torsion pendulum low-pass filter, two kinds of surface waves, Love and Rayleigh waves, have clearly appeared on the filtered records of N–S and E–W or U–D components separately. The dispersion curves of these two kinds of surface waves could be obtained from the filtered records at each observatory.

The velocities of successive waves were calculated according to $\Delta/(t_{ai}-t_0)$, or $\Delta/(t_{bj}-t_0)$, $(i, j=0, 1, 2, 3, \ldots)$ where $t_{ai}$ and $t_{bj}$ are the times of $a_i$ and $b_j$ as shown in Fig. 4 and $t_0$, $\Delta$ are the origin times and travel distances from the epicenter to each observational position measured along the great circles. The velocities thus obtained are the group velocities. An example of the dispersion curve is shown in Fig. 7, in which the upper and the lower curves correspond to the dispersion curves concerning the group velocities of Love and Rayleigh waves respectively. In this figure, several points enclosed by

dotted lines correspond to the excluded points already shown in Fig. 5.

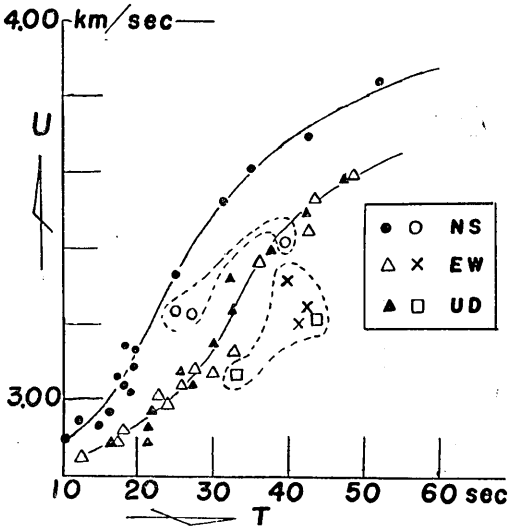


Fig. 7. An example of the dispersion curve obtained from the filtered seismograms of Hukuoka.

## 5. Classification of dispersion curves.

In the course of drawing these dispersion curves of Love and Rayleigh waves at each observational position and comparing them with each other, an interesting result was noticed that they can be classified into three groups, A, B and C, and moreover that the locations of observational positions which correspond to each of the dispersion curves are distributed systematically as in Fig. 8. In order to show that this classification is

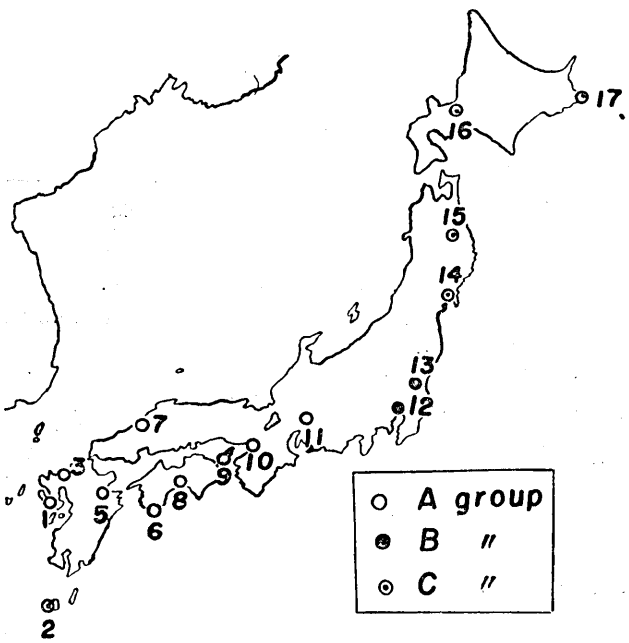


Fig. 8. The distribution of the observatories of three groups.

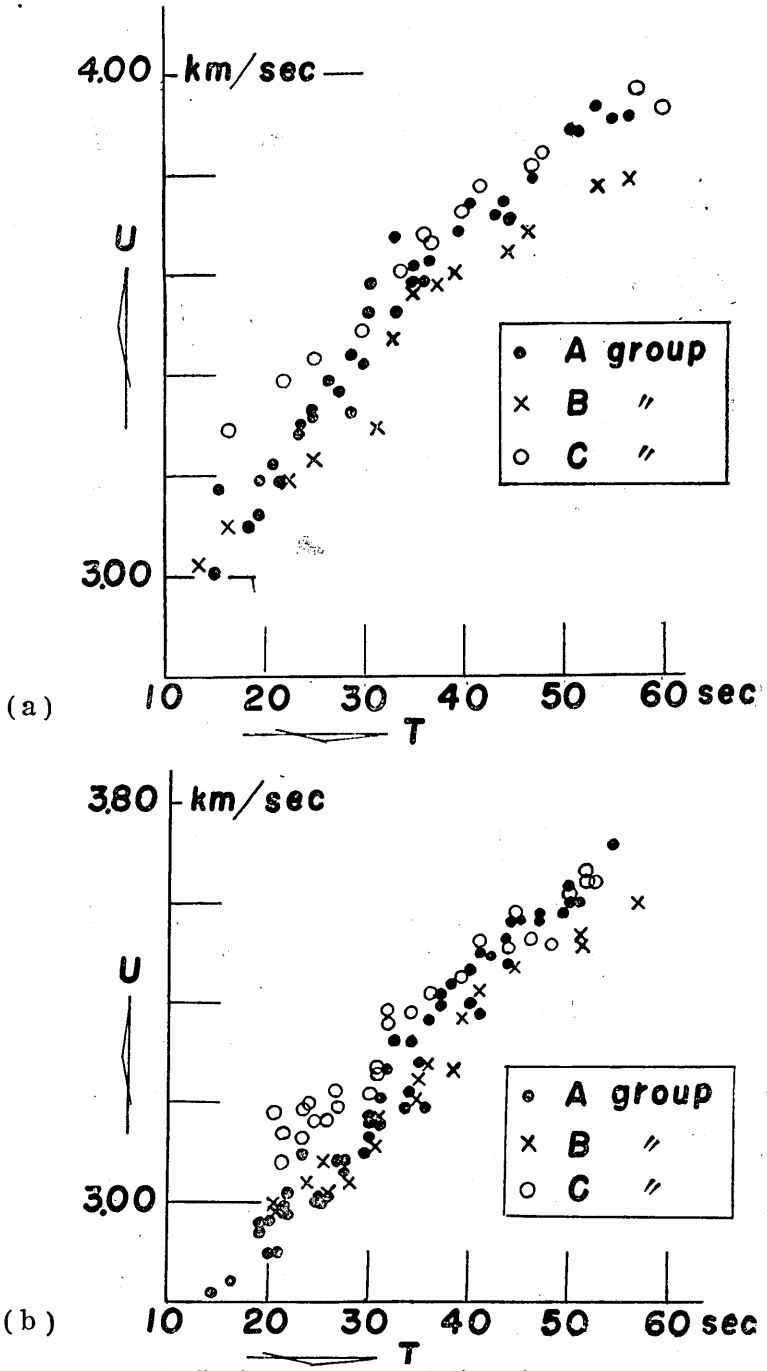


Fig. 9. The distribution of the dots of dispersion curves of three groups.

not an arbitrary one, Figs. 9-a and -b are given in which all data are plotted. From these two figures, together with Fig. 8, we can consider the classification to be neither artificial nor due to observational errors.

Fig. 10 shows the most probable dispersion curves of these three types and Figs. 11-a and -b were drawn in order to compare our curves with other dispersion curves of Love and Rayleigh waves having paths of various regions already obtained by many authors.

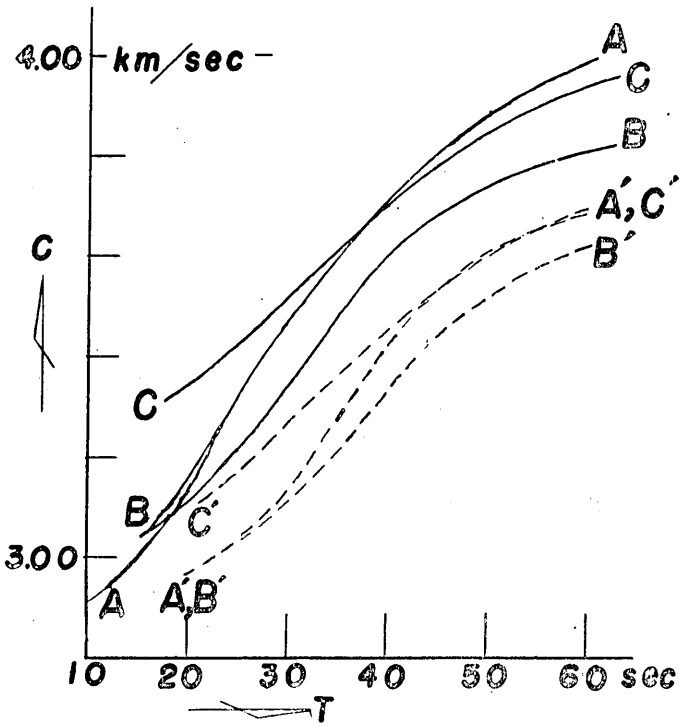


Fig. 10. The dispersion curves of three types.

Of these three types of dispersion curves, the writer refrains here from studying the *B* type on account of its being based on too scarce data. (It contains only two observational positions.) The difference of the remaining two types *A* and *C* are considered to be due to the difference in crustal structures through which the surface waves travelled. From Fig. 1, it is suggested that the differences stated above may be mainly due to the difference in crustal structures of Japan Sea and of East China Sea. In order to figure out the crustal structures in these two regions, the effect of the continental structure which is considered

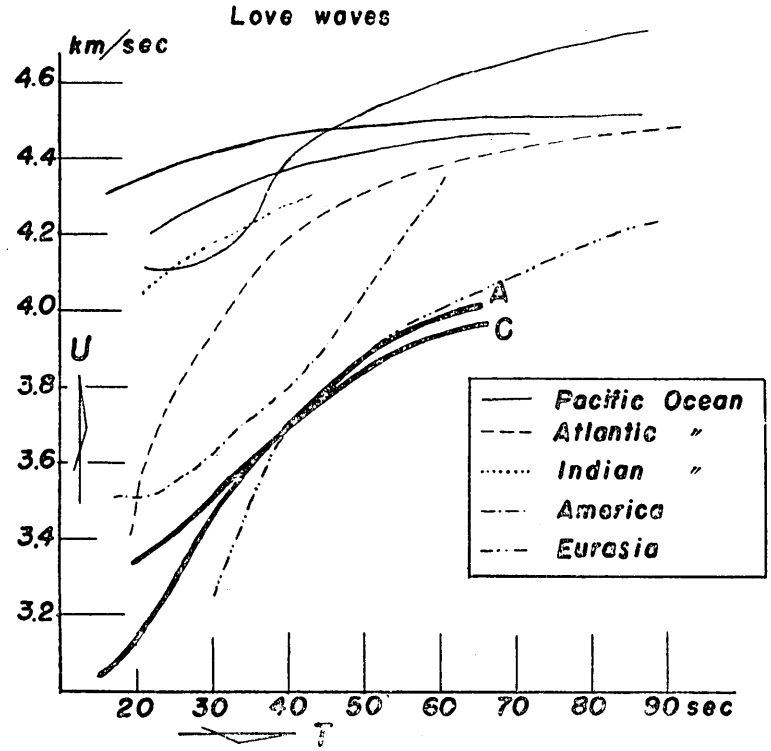


a.

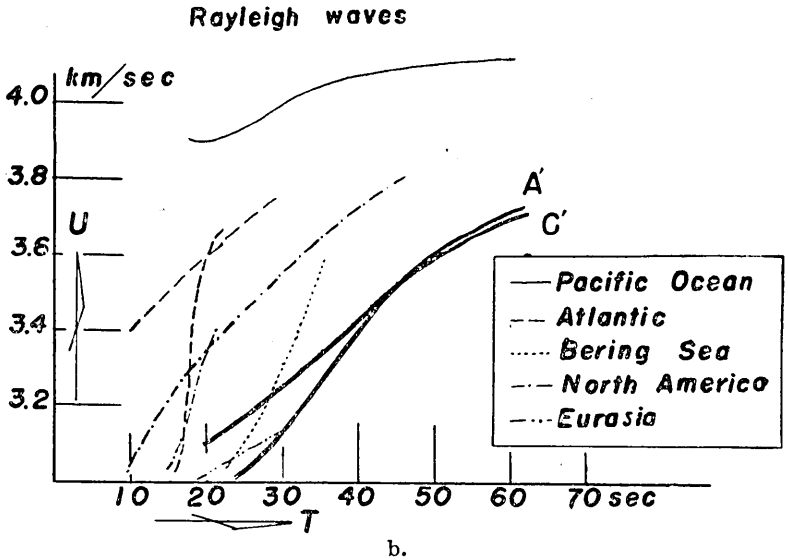


b.

Fig. 11. Comparison of the dispersion curves obtained with those by other authors of various travelling paths.

to be common to both of these two wave paths must be excluded from our two types of dispersion curves. But, unfortunately, on account of the lack of appropriate seismograms for this purpose, the writer had to be satisfied with studying here the mean crustal structure of (continent+Japan Sea) and of (continent+East China Sea).

## 6. Discussions on the estimation of crustal structure by a dispersion curve.

Y. Satô has published recently an interesting result of his theoretical study on the problem of estimating the crustal structure by the dispersion curve of Love waves[3]. He pointed out in his paper with numerical examples that the crustal structure cannot be uniquely determined by the dispersion curve of Love waves alone. It was shown by him,

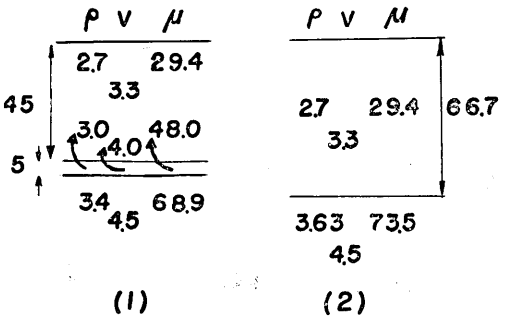


Fig. 12. Actual crustal structure (1) and equivalent crustal structure (2).

for instance, that the dispersion curve of Love waves due to a doubly layered crustal structure such as is illustrated in Fig. 12–1 is very similar, in the range of observational errors at least, to that due to a single-layered crustal structure such as is shown in Fig. 12–2. In other words, if we try to determine the crustal structure by the dispersion curve of Love waves alone, assuming a single layer, our estimation may be a wrong one, for instance, such as 2, while the actual crustal structure is as 1 in Fig. 12.

Though Satô's discussion is limited only to the case of Love waves, a similar result will be obtained in the case of Rayleigh waves.

The next problem which is quite interesting to solve mathematically is what would the respective results of estimated crustal structures turn out to be when we use the dispersion curve of Love waves

3) Y. SATÔ, *Bull. Earthq. Res. Inst.*, **29** (1951), 519.

and when we use that of Rayleigh waves both under the assumption of a single-layered structure for the two cases when the actual crustal structure is a single-layered one and when it is not; or in other words, the problem if the agreement of the respective results from the dispersion curve of Love waves and that from that of Rayleigh waves confirm the suitability of the assumption under which the estimation was made.

Though the theoretical conclusion of this problem will presently be given by Y. Satô, the writer would like to give the results of his examinations of estimating a crustal structure by using the dispersion curves of the two kinds of surface waves.

## 7. Estimation of the crustal structures using two dispersion curves for C groups.

At first, the crustal structure for (*c*) region was estimated under the assumption of a single layer using two kinds of dispersion curves $C$ and $C'$ of Love and Rayleigh waves.

The theoretical equation of dispersion curves, which is called a characteristic equation, of Love waves when a homogeneous semi-infinite medium is overlain by a homogeneous layer of thickness H is given as follows:

$$\tan\left\{\left(\frac{c^2}{v_1^2}-1\right)^{1/2}\frac{2\pi}{L}H\right\}=\frac{\mu_2}{\mu_1}\frac{\left(1-\frac{c^2}{v_2^2}\right)^{1/2}}{\left(\frac{c^2}{v_1^2}-1\right)^{1/2}}\cdots\cdots\cdots(1),$$

where $v_1$ and $v_2$ are the velocities of shear waves in the layer and in the semi-infinite medium, $\mu_1$ and $\mu_2$ the corresponding rigidities, $c$ and $L$ the phase velocity and wave length of Love waves respectively.

In order to apply this formula to our dispersion curve of Love waves concerning their group velocities $U$, the observed dispersion curve concerning the phase velocities $c$ was at first drawn by the formula

$$U=c-L\frac{dc}{dL}$$

which is a well-known relation between the group velocity $U$ and the phase velocity $c$ of dispersive waves.

By this $c\sim L$ curve, $v_1$ and $v_2$ were approximately estimated as 3.4 km/sec and 4.2 km/sec respectively as are seen from the trends of the

curves in Fig. 13. Then, a suitable pair of two parameters $\mu_2/\mu_1$ and $H$, by which the numerical relations between $c$ and $L$ obtained from the equation (1) agree with the observed curve of $c\sim L$, can be obtained from the same equation. Practically, however, not only one but a few suitable pairs of $\mu_2/\mu_1$, and $H$ are found. In our case, (1.6, 25 km); (1.8, 26 km); (1.9, 27 km) all seemed to be suitable for observational curve within observational errors at least. (See Table II).

Table II.

| $C$ | ($\mu_2/\mu_1=1.6$, $H=24$ km) | | ($\mu_2/\mu_1=1.8$, $H=26$ km) | | ($\mu_2/\mu_1=1.9$, $H=27$ km) | |
|---|---|---|---|---|---|---|
| | $L/H$ | $L$ | $L/H$ | $L$ | $L/H$ | $L$ |
| 4.1 km/sec | 10.0 | 240 km | 9.08 | 236 km | 8.67 | 234.0 km |
| 4.0 〃 | 5.76 | 138 〃 | 5.31 | 138 〃 | 5.12 | 139.0 〃 |
| 3.9 〃 | 4.35 | 105 〃 | 4.07 | 106 〃 | 3.96 | 107.0 〃 |
| 3.8 〃 | 3.30 | 79 〃 | 3.10 | 81 〃 | 3.05 | 82.5 〃 |
| 3.7 〃 | 2.54 | 61 〃 | 2.42 | 63 〃 | 2.38 | 64.4 〃 |
| 3.5 〃 | 1.18 | 28 〃 | 1.16 | 32 〃 | 1.15 | 31.0 〃 |

On the other hand, the same estimation can be done using the dispersion curve of Rayleigh waves with the same single-layered assumption.

The characteristic equation in this case is somewhat cumbersome, being as follows:

$$\begin{vmatrix} -\frac{f^2-s_2^2}{k_1^2}Y_2, & 2\frac{\mu_2}{\mu_1}\frac{ifs_2}{k_2^2}Y_1, & 0, & -2\frac{\mu_2}{\mu_1}\frac{ifs_2}{k_2^2}, & 0, & \frac{s_2 f}{k_2^2} \\ -\frac{f^2-s_2^2}{k_2^2}Y_1, & -2\frac{\mu_2}{\mu_1}\frac{ifs_2}{k_2^2}Y_2, & \frac{\mu_2}{\mu_1}\frac{f^2-s_2^2}{k_2^2}, & 0, & -\frac{if_1^2}{k_2^2}, & 0 \\ 2\frac{ifr_2}{h_2^2}X_1, & \left(2\frac{\mu_2}{\mu_1}\frac{r_2^2}{h_1^2}-\frac{\lambda_2}{\mu_1}\right)X_2, & -\frac{\mu_2}{\mu_1}\frac{2ifr_2}{h_2^2}, & 0, & \frac{r_2 f}{k_2^2}, & 0 \\ 2\frac{ifr_2}{h_2^2}X_2, & \left(2\frac{\mu_2}{\mu_1}\frac{r_2^2}{h_2^2}-\frac{\lambda_2}{\mu_1}\right)X_1, & 0, & \frac{\lambda_2}{\mu_1}-2\frac{\mu_2}{\mu_1}\frac{r_2^2}{h_2^2}, & 0, & -\frac{if^2}{h_2^2} \\ 0, & 0, & -\frac{f^2+s_1^2}{k_1^2}, & 2\frac{ifs_1}{k_1^2}, & \frac{if^2}{k_1^2}, & -\frac{sf^2}{k_1^2} \\ 0, & 0, & \frac{2ifr_1}{h_1^2}, & 2\frac{r_1^2}{h_1^2}-\frac{\lambda_1}{\mu_1}, & -\frac{r_1 f}{h_1^2}, & \frac{if^2}{h_1^2} \end{vmatrix} = 0 \quad (2),$$

where $r^2=f^2-h^2$, $s^2=f^2-k^2$, $h^2=\rho p^2/(\lambda+2\mu)$, $k^2=\rho p^2/\mu$, in which

$\lambda$, $\mu$, $\rho$= Lamés elastic constant and density,

$p=2\pi/T$,
$f=2\pi/L$,
$T$, $L$=period and wave length of Rayleigh waves,

and $X_1=\cosh r_2H$, $X_2=\sinh r_2H$, $Y_1=\cos s_2H$, $Y_2=\sin s_2H$. Suffix 1, 2, except those of $X$ and $Y$, correspond to that of superficial layer and of semi-infinite medium respectively[4].

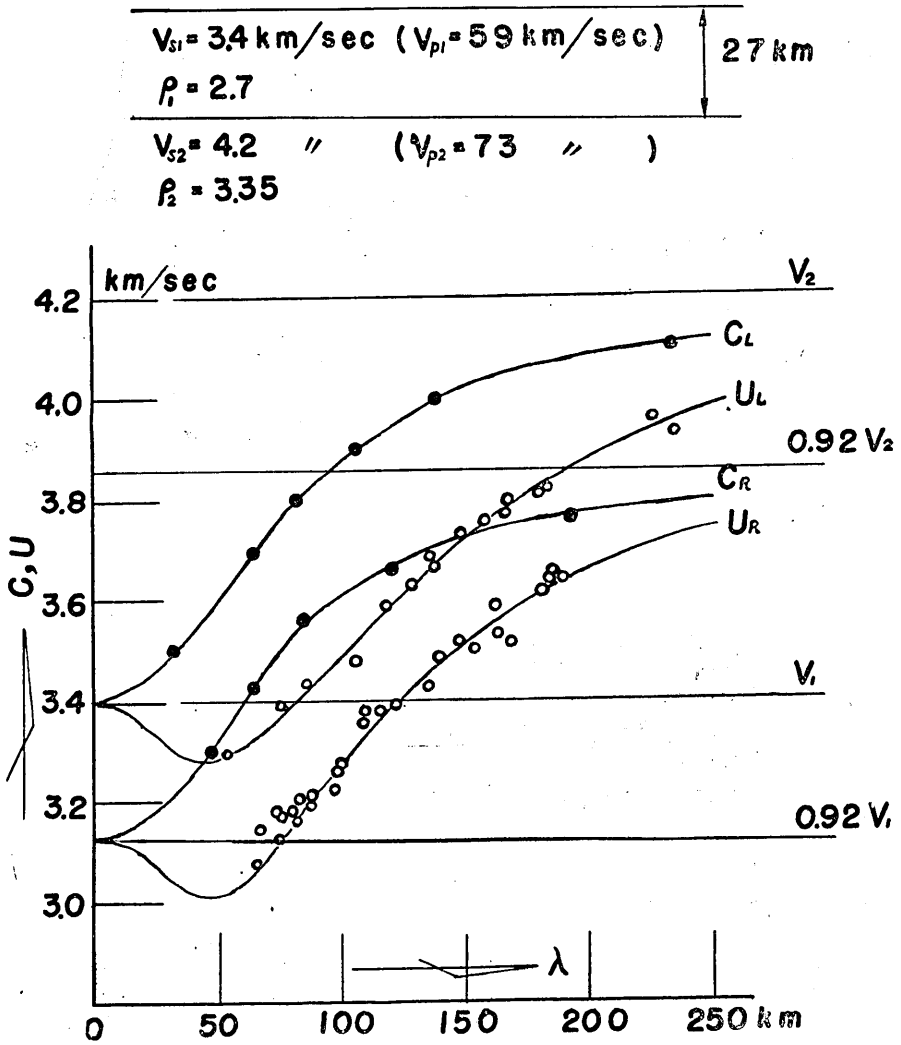


Fig. 13. The estimated crustal structure of (c) ragion and the results of theoretical calculations (filled circle).

4) K. SEZAWA. *Bull. Earthq. Res. Inst.*, **3** (1927), 1.

Putting $\lambda_1=\mu_1$, $\lambda_2=\mu_2$ and substituting $u$ (the velocity of P-waves) and $v$ (the velocity of S-waves) for $\lambda s$ considering that $u^2=(\lambda+2\mu)/\rho$, $v^2=\mu/\rho$, the theoretical curves between the phase velocity $c$ and the wave length $L$ of Rayleigh waves can be obtained with parameters $\mu_2/\mu_1$ and $H$ from the equation (2). The practical calculations were performed transforming the equation (2) into a form more convenient for numerical calculations.

The writer's purpose was to find out if any pair of $\mu_2/\mu_1$ and $H$ already obtained in the case of Love waves is also appropriate for the equation (2) to fit the observational curve of Rayleigh waves. The result was quite interesting. The pair of $\mu_2/\mu_1=1.9$ and $H=27$ km was his result, that is, if we assume the crustal structure of (*c*) region as a single-layered one and take the ratio of rigidity of the upper layer and of the lower medium as 1.9 and the thickness of the layer as 27 km, our observational dispersion curves agree quite well with the theoretical dispersion curves both on Love and Rayleigh waves. This result is shown in Fig. 13, in which $U_L$ and $U_R$ are the dispersion curves concerning the group velocities of Love and Rayleigh waves drawn by the observational data represented by hollow circles, $C_L$, $C_R$ are the curves concerning the corresponding phase velocities and the dots marked by filled circles represent the calculated data indicated in Table III. If we take the density of the upper layer at 2.7 gr./cm$^3$, the estimated crustal structure of (*c*) region becomes as shown in the same figure.

Table III.

| Love waves | | | Rayleigh waves | | |
|---|---|---|---|---|---|
| $C$ | $L/H$ | $L$ | $C$ | $(2\pi/L)H$ | $L$ |
| 3.5 km/sec | 1.15 | 47.0 km | 3.3 km/sec | 1.14 | 47.0 km |
| 3.7 〃 | 2.38 | 64.4 〃 | 3.43 〃 | 0.84 | 64.4 〃 |
| 3.8 〃 | 3.05 | 82.5 〃 | 3.56 〃 | 0.64 | 84.0 〃 |
| 3.9 〃 | 3.96 | 107.0 〃 | 3.66 〃 | 0.45 | 120.0 〃 |
| 4.0 〃 | 5.12 | 139.0 〃 | 3.76 〃 | 0.28 | 192.0 〃 |
| 4.1 〃 | 8.67 | 234.0 〃 | | | |

The next study was for the dispersion curves of *A* group. In this case, the velocities of shear waves in the upper layer and in the lower medium were approximately estimated at 3.2 km/sec and 4.2 km/sec from $C_L$ and $C_R$ curves in Fig. 14. Considering that the velocity of

shear waves in the upper layer 3.2 km/sec in this case is smaller than that in *C* group, while that in the lower medium is the same, it seems rather natural to consider that in (*a*) region another superficial layer exists over the upper layer in (*c*) region, which means the crustal structure is a double-layered one. But, in order to see if there is a

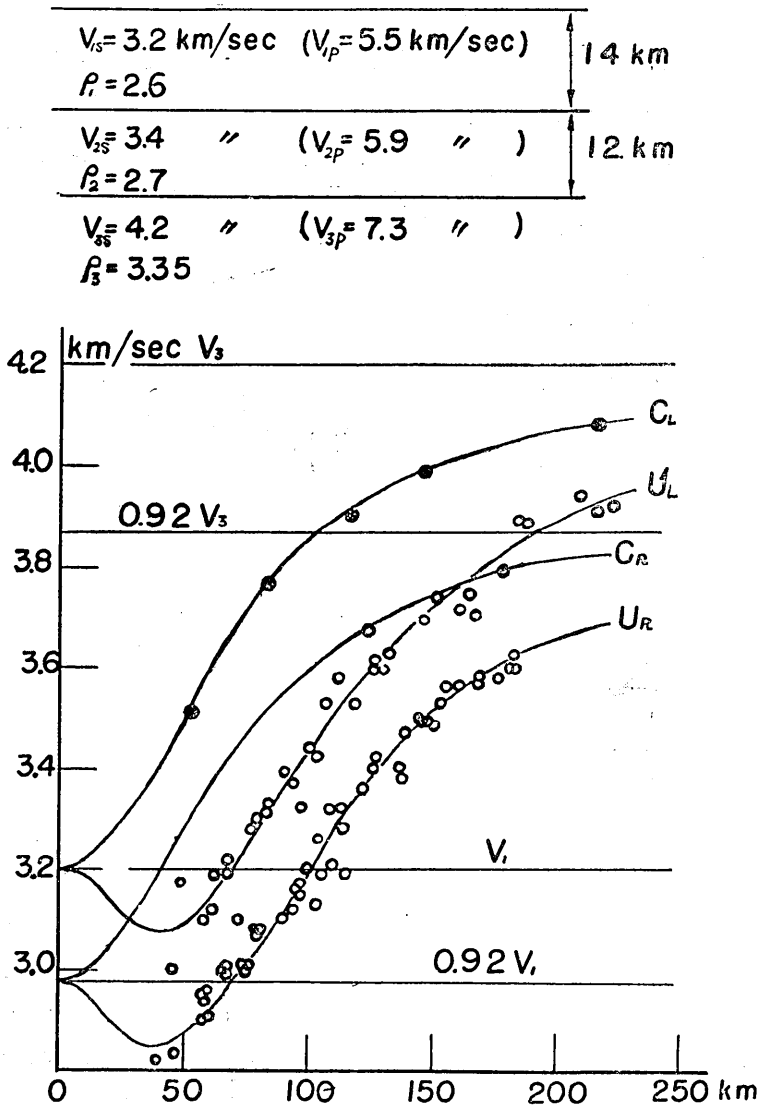


Fig. 14. The estimated crustal structure of (a) region and the results of theoretical calculations (filled circle).

case when the suitable values of $\mu_2/\mu_1$ and $H$ for Love waves dispersion curve are not suitable for Rayleigh waves dispersion curve when we assume a single-layered structure, the writer tried at first to estimate the crustal structure of this region also under the assumption of a single layer. The method is quite the same as for the case of $C$ group already described. The result was as follows: the suitable pairs of $\mu_2/\mu_1$ and $H$ for Love waves, estimated at (2.4, 22 km) or (2.2, 22 km), were, as is shown in Fig. 15, not suitable for Rayleigh wave's dispersion curve. In other words, the writer could not find any suitable quantities concerning the crustal structure which satisfy both of the two dispersion curves obtained observationally for Love and Rayleigh waves, so far as he assumes a single-layered structure in this region.

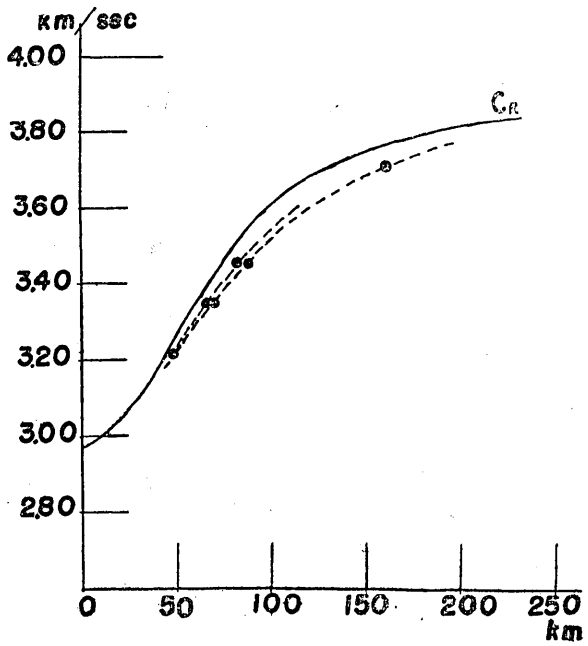


Fig. 15.

If the results for (*c*) regions already obtained are considered, it may be natural to assume here such a crustal structure as are illustrated in Fig. 16. Under this assumption, the next calculations were made. Now we must find the thickness of the 1st and the 2nd layer $H_1$ and $H_2$.

The characteristic equation of Love waves for doubly stratified medium is as follows:

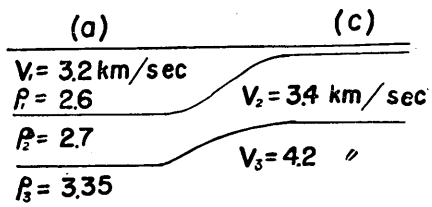


Fig. 16.

$$D \equiv D^c + D^s = 0 \qquad (3)$$

where

$$D^c/\mu_2^2 f^2 \equiv \mathfrak{A}_2 \cos\{\xi h_1 \mathfrak{A}_1\}\,[-\chi_{32}\mathfrak{A}\cos\{\xi h_2 \mathfrak{A}_2\} + \mathfrak{A}_2 \sin\{\xi h_2 \mathfrak{A}_2\}]$$

$$D^s/\mu_2^2 f^2 \equiv \chi_{12}\mathfrak{A}\sin\{\xi h_1 \mathfrak{A}_1\}\,[\chi_{32}\mathfrak{A}\sin\{\xi h_2 \mathfrak{A}_2\} + \mathfrak{A}_2 \cos\{\xi h_2 \mathfrak{A}_2\}]$$

in which

$$\mathfrak{A}_k \equiv \sqrt{(r_k^2 \mathfrak{V}^2 - 1)}\ , \qquad k=1,\ 2,\ 3$$

$$\mathfrak{A} \equiv \sqrt{(1-\mathfrak{V}^2)}\ ,$$

$$\mathfrak{V}_k \equiv c/v_k\ , \qquad k=1,\ 2,\ 3$$

$$v \equiv v_3\ ,$$

$$r_k \equiv v_3/v_k\ , \qquad k=1,\ 2$$

$$\xi \equiv fH\ ,$$

$$\chi_{jk} \equiv \mu_j/\mu_k\ ,$$

$$f \equiv 2\pi/L\ ,$$

where $c$ is the phase velocity of Love waves while other notations are illustrated in Fig. 17[5].

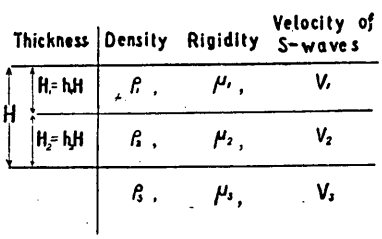


Fig. 17.

Putting $v_1=3.2$ km/sec, $v_2=3.4$ km/sec, $v_3=4.2$ km/sec, $\rho_1=2.6$, $\rho_2=2.7$, $\rho_3=3.35$, and accordingly, $\chi_{12}=0.852$, $\chi_{32}=1.888$ in the above equation, we can find suitable values of $H_1$ and $H_2$ from the equation (3) which fit the equation to the $C$ curve in Fig. 14.

5) Y. SATÔ. *loc. cit.*

The results are given in Table IV and the data are shown in Fig. 14 by filled circles, which shows how these data given above obtained under the assumption of doubly stratified structure agree with the observational data in this region. The crustal structure of ($a$) region thus estimated from the dispersion curve of Love waves are illustrated in the same figure.

Table IV.

| $C$ | $L$ ($H_1$=14 km, $H_2$=12 km) |
|---|---|
| 3.52 km/sec | 52.5 km |
| 3.76 〃 | 89.0 〃 |
| 3.90 〃 | 117.0 〃 |
| 3.98 〃 | 147.0 〃 |
| 4.01 〃 | 198.0 〃 |

There remains the next work to be done. That is to see if these values of $H_1$=14 km and $H_2$=12 km obtained from the Love waves dispersion curve are also suitable for that of Rayleigh waves. But numerical calculations of theoretical dispersion curve of Rayleigh waves in the case of double layers are so cumbersome that the writer has not yet completed this work.

## 8. Conclusions.

Though a few theoretical studies must be completed before the writer gives any conclusion from his study given above, it may be said at least that there exists an obvious difference of crustal structure between Japan Sea and East China Sea. Moreover, if we consider that the length of the travelling paths of waves in Japan Sea and in East China Sea was approximately 25% and 35% of the whole travelling length, the difference of crustal structure given above will become ever more larger when the effect of the continental path is excluded from the dispersion curves. And if a further presumption is permitted, we may imagine the following figure on the crustal structure of our regions, that is, the crustal structure of both continents and East China Sea is a double-layered one while in Japan Sea regions, the structure is a single-layered one and in which the middle layer appears at the surface, or if the uppermost layer exists, it is quite thin.

There remain two points to be considered in this investigation, that is,

1) What does the reappearance of somewhat longer period waves in the filtered records of almost all the observational position mean? (See Fig. 5)

2) Has the difference of dispersion curves of *B* group from those of *A* and *C* on which the writer hesitated to consider on account of their too scarce data any geophysical meaning?

Of these two points the writer will treat in the next opportunity.

In conclusion, the writer wishes to express his sincere thanks to S. Miyamura who gave him many advices and encouragements in the course of his works and to Y. Satô who gave him kindly instructions in numerical calculations.

The expense of the present study was partly defrayed from the Fund of the Scientific Research from the Ministry of Education.

---

## 21. 1950年8月15日のアッサム大地震の表面波の分散曲線について

地震研究所　秋　間　哲　夫

1950年8月15日にインドのアッサム地方で起つた大地震の國内における地震記象の中から20点ばかりをえらんで，それを各成分毎に振り振子を利用した低域濾波器にかけて長周期の波だけにして調べて見ると，極めて明瞭にラヴ波とレーリー波とが夫々南北成分，及び東西，上下成分に分離して観測出來た．そこで，各点毎にラヴ波，レーリー波に關する分散曲線を作つて見ると，之等の分散曲線が東北日本のものと西南日本のものとで之またかなり明瞭に相異していることが認められた．そこでこの二つの型の分散曲線から，震源から大陸を渡り，日本海を通つて東北日本に達する部分と同じく大陸を通り，東支那海を通つて西南日本に達する部分との地殻構造を求めて見ると，前者に於ては厚さ 27 km の單一戸，後者に於ては，厚さ 14 km と 12 km より成る二重戸を考えると，共にラブ波とレーリー波の分散曲線の何れにも夫々の分散曲線の理論式がよくあてはまることが分つた．

從來から表面波を用いて地下構造を求めることは，多くの人達によつてしばしばやられているけれ共，殆んどすべてのものが，ラヴ波乃至はレーリー波の分散曲線の一方だけから求めており，しかも單一戸と云う假定のもとに構造が求められている．しかしそうすると，佐藤泰夫氏の理論的研究でも分る様に，もし實際の地下構造が例えば二重戸だつたとすると，實際とは大分異つた物理常數と厚さとをもつた單一戸の地下構造が求められてしまう危險が生ずる．

筆者の場合には幸いにしてラヴ波とレーリー波の兩方の分散曲線が得られたので，その兩者から地下構造をきめた．その点ではこゝにえられた結果は，少くとも從來のこの種の試みよりは高い信用度がおけるのではないかと思う．

---